

Treatment of boundary conditions in three-dimensional large eddy simulations of calorically perfect gas detonations

B. Maxwell^{1,2} and W.-H. Wang²

¹Department of Mechanical Engineering, University of Ottawa, Ottawa, Ontario, Canada

²Department of Mechanical and Aerospace Engineering, Case Western Reserve University
Cleveland, Ohio, USA

1 Introduction

To date, a vast majority of multi-dimensional numerical simulations of detonation waves have relied on solving Euler's equations of fluid motion, which fundamentally assumes inviscid flow behavior. That is, solving Euler's equations does not account for turbulent mixing, molecular diffusion, or boundary layer effects near walls. While many investigations have not successfully captured *exact* experimental observations, some have been able to show that, with sufficient resolution, regular and mildly irregular detonation structures at near-CJ velocities are recovered quite well, at least qualitatively [1–3]. For much higher global activation energies, i.e., increased irregularity, solving the Euler equations have only yielded limited success [4]. It was found that although Euler simulations can provide limited insight into the roles that shock compression or turbulent motions may have on detonation propagation, the solutions obtained for high activation energies were subject to changes in resolution and did not converge to unique solutions [4].

Two-dimensional direct numerical simulations (DNS) of the Navier-Stokes equations addressed this problem by attempting to resolve the full spectrum of scales present, which included viscous and molecular diffusion effects. Such investigations [5–9] have revealed that practically attainable resolutions, in many full-scale two-dimensional problems, are insufficient to capture the correct reaction rates of shocked reactive gas and the corresponding cellular structure. What was found, however, was that physical diffusion is important to consider at high resolution when numerical diffusion becomes negligible [5]. In fact, we have previously demonstrated that closure of turbulent mixing rates plays a major role in determining the detonation cell size [10], especially for methane-based high activation energy mixtures. Using the compressible linear eddy model for large eddy simulation (CLEM-LES) for a calorically perfect gas equation of state, and using a one-step combustion model, it was found that providing closure to the turbulent mixing rates can permit the establishment of the correct expected cellular pattern when compared to experiments. However, no-slip boundary conditions and associated losses due to boundary layers were not accounted for. Thus, experimentally observed velocity deficits and their additional impact on the cellular pattern were not recovered. When the CLEM-LES approach was developed, the turbulent diffusivity (mixing rates), and the dissipation rates were formulated in terms of the *Kolmogorov* number, C_κ . Typically, C_κ is estimated from experiments to be ~ 1.5 , however published values range anywhere from 1.2 to 4 [11]. In fact, we found that the cellular structure of the detonation wave was heavily influenced by the *tuning* of C_κ , and is how we concluded that not only are detonation waves controlled by the chemical reaction rate and its sensitivity to compressibility of the gas, but is also heavily influenced by the rates of turbulent mixing [10]. In our past-work, however, we mostly investigated two-dimensional situations without momentum or energy losses, and in order to

capture experimentally observed cellular structures, a C_κ value of 6.7 was required. Since then, we have treated C_κ as a tuning parameter.

In the current work, we revisit the application of the CLEM-LES for a calorically perfect gas detonation in an attempt to clarify the role of the Kolmogorov number, and whether or not it should be treated as a tuning parameter. We perform three-dimensional simulations of detonation propagation in methane–oxygen, in a thin-channel, and also include no-slip walls as boundary conditions. Instead of tuning the Kolmogorov number to obtain the desired cell size, as we’ve done in the past, we instead use a standard value of 1.5 and compare to experiments accordingly.

2 Numerical Approach

For the highly compressible and transient flow at hand, the governing Navier-Stokes equations are filtered using the large eddy simulation (LES) methodology. For a calorically perfect gas, the conservation equations for mass, momentum, energy, and subgrid kinetic energy are:

$$\frac{\partial \bar{\rho}}{\partial t} + \nabla \cdot (\bar{\rho} \tilde{\mathbf{u}}) = 0 \quad (1)$$

$$\frac{\partial \bar{\rho} \tilde{\mathbf{u}}}{\partial t} + \nabla \cdot (\bar{\rho} \tilde{\mathbf{u}} \otimes \tilde{\mathbf{u}}) + \nabla \bar{p} - \nabla \cdot \bar{\rho} (\nu + \nu_t) \left(\nabla \tilde{\mathbf{u}} + (\nabla \tilde{\mathbf{u}})^T - \frac{2}{3} (\nabla \cdot \tilde{\mathbf{u}}) \hat{\mathbf{I}} \right) = 0 \quad (2)$$

$$\frac{\partial \bar{\rho} \tilde{e}}{\partial t} + \nabla \cdot \left((\bar{\rho} \tilde{e} + \bar{p}) \tilde{\mathbf{u}} - \tilde{\mathbf{u}} \cdot \bar{\boldsymbol{\tau}} \right) - \left(\frac{\gamma}{\gamma - 1} \right) \nabla \cdot \left(\bar{\rho} \left(\frac{\nu}{Pr} + \frac{\nu_t}{Pr_t} \right) \nabla \tilde{T} \right) = -Q \bar{\omega} \quad (3)$$

$$\frac{\partial \bar{\rho} k^{\text{sgs}}}{\partial t} + \nabla \cdot (\bar{\rho} \tilde{\mathbf{u}} k^{\text{sgs}}) - \nabla \cdot \left(\frac{\bar{\rho} \nu_t}{Pr_t} \nabla k^{\text{sgs}} \right) = \bar{\rho} \nu_t \left(\nabla \tilde{\mathbf{u}} + (\nabla \tilde{\mathbf{u}})^T - \frac{2}{3} (\nabla \cdot \tilde{\mathbf{u}}) \hat{\mathbf{I}} \right) \cdot (\nabla \tilde{\mathbf{u}}) - \bar{\rho} \epsilon, \quad (4)$$

where ρ , p , e , T , \mathbf{u} , and k^{sgs} refer to density, pressure, specific sensible + kinetic energy, temperature, velocity vector, and subgrid kinetic energy, all of which are normalized by the quiescent reactive mixture properties, see [10]. Other usual properties to note are the heat release, Q , the ratio of specific heats, γ , the kinematic viscosity, ν , the dissipation rate, ϵ , the viscous shear stress tensor, $\boldsymbol{\tau}$, the Prandtl number, Pr , the chemical reaction rate, $\bar{\omega}$, and the identity matrix, $\hat{\mathbf{I}}$. The subscript ‘t’ refers to a turbulent quantity. \bar{f} represents a spatially averaged value of f , and Favre-average (LES) filtering is achieved through $\tilde{f} = \bar{\rho} f / \bar{\rho}$, where f represents one of the many state variables (ρ , p , e , T , \mathbf{u} , and k^{sgs}). The turbulent viscosity and dissipation are modelled according to

$$\nu_t = \frac{1}{\pi} \left(\frac{2}{3C_\kappa} \right)^{3/2} \sqrt{k^{\text{sgs}}} \bar{\Delta} \quad \text{and} \quad \epsilon = \pi \left(\frac{2k^{\text{sgs}}}{3C_\kappa} \right)^{3/2} / \bar{\Delta}. \quad (5)$$

Here, $\bar{\Delta}$ is the minimum grid spacing (which corresponds to the LES filter size), and C_κ is the *Kolmogorov* number. Treatment of near-wall turbulence is provided through the wall modelling approach of Kawai and Larson [12]. Then, like in any other reactive LES approach, the chemical reaction source term, $\bar{\omega}$, requires closure. This is achieved using the CLEM sub-grid modeling strategy [10] which includes first order one-step Arrhenius chemical kinetics. We use the same model parameters as our previous work [10] to simulate detonations in premixed methane–oxygen ($\text{CH}_4 + 2\text{O}_2$ at $p_o = 3.5$ kPa), with the exception of the Kolmogorov number, which we intentionally set to a standard accepted value of $C_\kappa = 1.5$. The LES filter size was varied to study the effects of LES grid resolution, while a minimum LEM subgrid resolution of $19.5 \mu\text{m}$ was used for all simulations. This subgrid resolution was previously found to resolve laminar flame structures behind shock strengths corresponding to $0.7 M_{\text{CJ}}$, see [10].

The three-dimensional numerical domain simulated was $x = 9\text{m}$ long with a $25\text{mm} \times 100\text{mm}$ cross section in the y and z directions, respectively. This length was chosen to permit a quasi-steady evolution of the detonation wave to form, and for turbulence statistics to be collected. The cross sectional geometry

corresponded to the experiments of Kiyanda and Higgins [13], for which schlieren diagnostics and wave velocity measurements have been obtained. To initiate the wave, an over-driven ZND profile was placed in the first 200 mm of the domain, with an overdrive factor of $f = 1.2$. All boundary conditions were specified to be no-slip wall conditions.

3 Quantitative and Qualitative Comparison to Experiment

Upon initiation of the detonation wave in each simulation, we first measured the wave speed as a function of time in the x -direction, along the geometric centre of the domain. For averaging of the unsteady wave velocity, we discard measurements before the first 0.001 s of the simulation. This is to allow the over-driven wave to settle to a quasi-steady average velocity, which was below the CJ-velocity of $M_{CJ} = 6.30$ in all cases. A summary of detonation velocities obtained using other LES-filter sizes is shown in table 1. In general we found an increasing trend in average detonation velocity by decreasing the LES-filter size. However, as we approached $\bar{\Delta} = 0.3125$ mm, the average detonation velocity changed by only 1.3% when compared to $\bar{\Delta} = 0.625$ mm. We also note that for cases where $\bar{\Delta} > 0.625$ mm, only a short window of measurements was possible prior to eventual failure of the detonation wave. In these cases, the detonation velocities obtained were not sufficient to permit a self-sustained and quasi-steady propagation of the detonation wave.

Also shown in table 1 are the experimentally measured detonation wave velocities in both Kiyanda and Higgins [13], and also our previous experiments [10] which had double the domain height and a slightly smaller cross section at only 19 mm. We note that by specifying no-slip boundary conditions, a sufficient momentum loss is introduced causing the wave to propagate with a steady velocity deficit. In Kiyanda and Higgins, the detonation velocity was measured to be $M_{CJ} = 5.53$, while our simulated velocity was found to be comparable, but slightly lower at $M_{CJ} = 5.22$ for $\bar{\Delta} = 0.625$ mm or $M_{CJ} = 5.29$ for $\bar{\Delta} = 0.3125$. We attribute this $\sim 5\%$ difference to slightly larger diffusion coefficients in the simulation compared to real values, owing to the necessary scaling to permit post-shock flames to propagate at the correct speed using our perfect gas assumption and one-step modelling strategy. Despite this difference, we demonstrate that by specifying no-slip boundary conditions, and thus accounting for the momentum loss due to boundary layers, the current simulation is a significant improvement on our previous two-dimensional simulations [10], which were always found to propagate within 1% of the CJ-velocity.

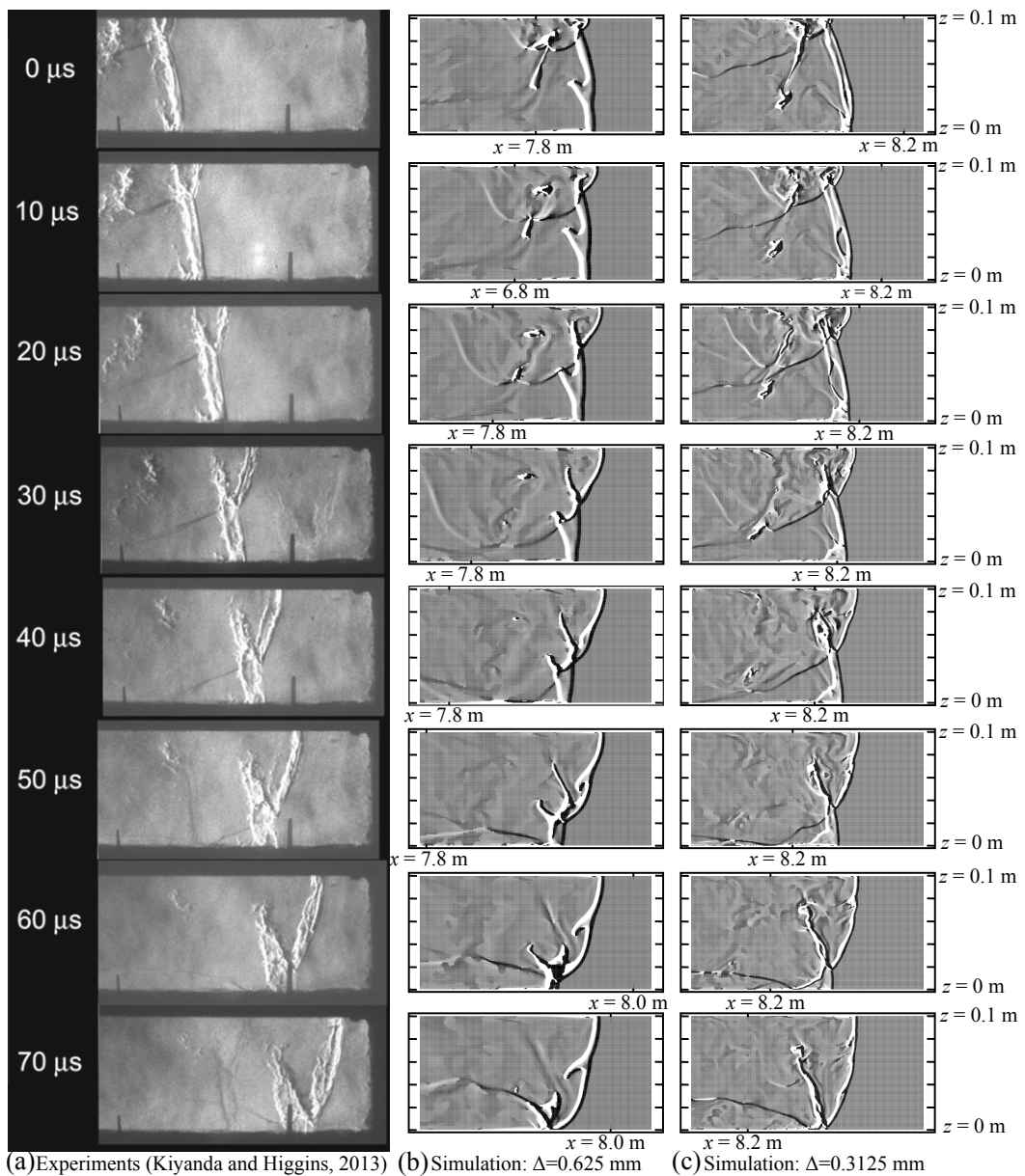
A direct comparison of numerical schlieren images for $\bar{\Delta} = 0.625$ mm and $\bar{\Delta} = 0.3125$ mm to experimentally obtained schlieren images [13] is shown in figure 1. Both the experimental and simulation images are shown to the same scale and time intervals between frames. Both simulations have a remarkable qualitative agreement with the experiment, especially for $\bar{\Delta} = 0.3125$ mm where finer details are resolved. Both filter sizes compare well to experiments in terms of the cell size, the decoupling dynamics of the reaction zone from the incident shock, the formation of an unburned tongue and pockets of reactive gas, and location of the transverse shock waves.

4 Energy Density Spectrum

In order to gain some further insight into the turbulent nature of the detonation wave simulated, turbulent statistics were collected along the geometrical center of the domain cross section ($y = 12.5$ mm and $z = 50$ mm), in the x -direction. Specifically, velocity fluctuations u' , v' , and w' were measured along this line, using the shock location as a reference point, and the energy spectrum was constructed accordingly. To measure u' , however, we first obtain the average velocity profile in the x -direction. For each instance in time considered, we first locate the position of the incident shock wave, where the density increases by 10%. From this, the u velocities are superimposed for each instance in time and averaged accordingly, using the shock location as a reference. For example, figure 2a shows the an instantaneous $u(x, t)$ -velocity field and the ensemble-averaged $u(x)$ -velocity field, for $\bar{\Delta} = 0.625$ mm, where the shock

Table 1: Quasi-steady detonation velocities (M_D) obtained using different LES-filter sizes ($\bar{\Delta}$).

$\bar{\Delta}$	M_D before failure	M_D/M_{CJ}	% change	detonation failure?
2 mm	4.51	0.72	-	yes
1.25 mm	4.98	0.79	10.4%	yes
0.625 mm	5.22	0.83	4.8%	no
0.3125 mm	5.29	0.84	1.3%	no
Kiyanda and Higgins [13]	5.53	0.88	-	no
Maxwell et al. (LES) [10]	6.35	1.01	-	no
Maxwell et al. (exp) [10]	5.19	0.82	-	no

**Figure 1:** Comparison of (a) schlieren images from [13] to (b & c) numerical schlieren images (density gradients) obtained from simulations at a cross-section corresponding to $y = 12.5$ mm for $\bar{\Delta} = 0.625$ mm and 0.3125 mm.

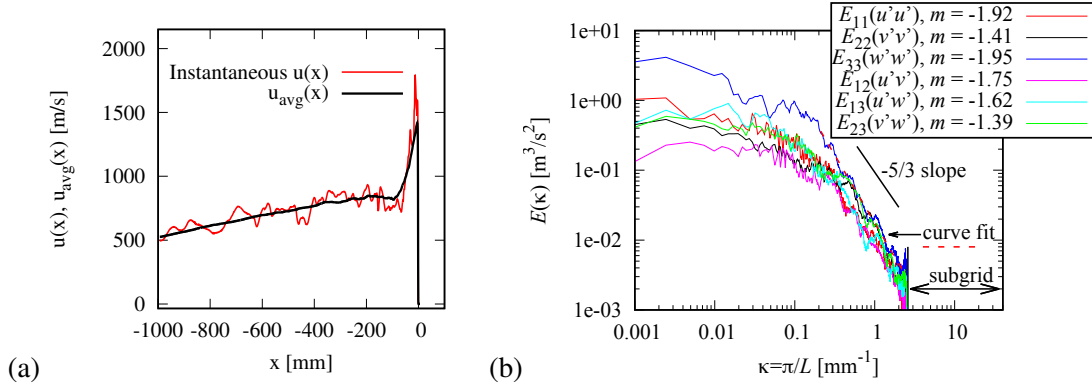


Figure 2: (a) Average and instantaneous velocity fluctuations in the x -direction, in the shock-frame of reference, and (b) the energy spectrum obtained for all velocity fluctuation correlation components for $\bar{\Delta} = 0.625$ mm. The -5/3 slope is indicated for reference.

location is used as the reference location. In total, 200 instances in time were averaged together to obtain the average u -velocity from which to obtain the instantaneous velocity fluctuation, u' . Once u' , v' , and w' were obtained, the energy spectrum was calculated for each of the 200 instances in time. This was done by applying the Fast-Fourier Transform (FFT) algorithm of [14] to the spatial statistical data for velocity correlation, $R_{i,j}(x) = u'_i(x)u'_j(x)$, to determine the respective energy density spectra at given wave numbers, and using the incident shock location as the frame of reference. This is in contrast to the past work of [15], where turbulent statistics of detonation wave-turbulence interactions were collected temporally at fixed laboratory frame of reference locations.

Once the energy spectrum was obtained for each instance in time, they were ensemble-averaged together, and is shown in figure 2b. Also shown in the figure, for reference, is the -5/3 slope, which is the power-law associated with the transfer of large scale turbulent kinetic energy to smaller scales through the incompressible and isotropic Kolmogorov *energy cascade*. Despite the compressible nature of detonation waves, it appears that the transfer of energy density tends to follow the -5/3 power-law, for all i,j components, for $\kappa > 0.2$ mm^{-1} . To confirm, the power spectra for each component, in this range of κ , was curve fit to a power law. The corresponding exponential dependence, m , is indicated for each component in the figure. In general, the rate of decay was found to be within $\sim 1/3$ of the theoretical -5/3 slope. Also, each of the different spectra were found to collapse onto each other at high wave numbers, with the exception of the $E_{33}(\kappa)$ spectrum. At low wave numbers, $\kappa < 0.1$ mm^{-1} , we found that $E_{33} > E_{11} > E_{22}$. This suggests that at low wave numbers, the thinness of the domain restricts kinetic energy fluctuations in the y -direction. As a result, most of the kinetic energy lies in the x - z plane. We believe kinetic energy is thus transferred to the z -direction through shearing of the flow involving the w' -Reynolds stress components. The significant velocity fluctuations in the z -direction are then transferred to higher wave numbers accordingly. We do note, however, that the total kinetic energy for the bulk u^2 -component is actually much greater than its fluctuating component, owing to the fact that there is significant average forward motion of the gas behind the shock. The non-zero magnitude of the energy spectra associated with the Reynolds stress components further suggests that the turbulence cascade is in fact not isotropic [16].

5 Conclusions

In this work, we revisited the application of the compressible linear eddy model for large eddy simulation (CLEM-LES) to a calorically perfect gas detonation, in methane-oxygen, and attempted to clarify whether the Kolmogorov number should be treated as a model constant, or a tuning parameter. We used past model parameters for the CLEM-LES [10], but extended to three-dimensions with no-slip wall

boundary conditions. We found that by doing so, and using a standard value for the Kolmogorov number ($C_\kappa = 1.5$) instead of tuning the value to desired results, we were able to capture the corresponding experimental wave velocity [13] to within 5%, while also capturing the corresponding cellular structure. This is a significant improvement on our past implementation of CLEM-LES to simulate methane–oxygen detonations, which did not account for no-slip wall conditions, nor capture the experimental velocity deficit (16% below CJ), and required tuning of C_κ to develop the desired cellular structure.

Finally, upon constructing the resulting energy spectrum of the simulation, using the incident shock location as a frame of reference, we found that the kinetic energy cascade (transfer of large scale turbulence to small scales) follows the well-known $-5/3$ power law description of incompressible turbulence in the inertial subrange, albeit not symmetric in every direction. The thinness of the channel was found to restrict velocity fluctuations in the y -direction at low wave numbers. This was found to lead to increased velocity fluctuations in the z -direction at all wave numbers. Also, the non-zero energy density associated with the Reynolds stress contributions, at high wave numbers, suggest the turbulence is in fact not isotropic.

This research was enabled in part by high performance computing resources provided the Core Facility for Advanced Research Computing at Case Western Reserve University.

References

- [1] V. N. Gamezo, D. Desbordes, and E. S. Oran, “Two-dimensional reactive flow dynamics in cellular detonation waves,” *Shock Waves*, vol. 9, pp. 11–17, 1999.
- [2] G. J. Sharpe, “Transverse waves in numerical simulations of cellular detonations,” *J. Fluid Mech.*, vol. 447, pp. 31–51, 2001.
- [3] G. Cael, H. D. Ng, K. R. Bates, N. Nikiforakis, and M. Short, “Numerical simulation of detonation structures using a thermodynamically consistent and fully conservative reactive flow model for multi-component computations,” *Proc. R. Soc. A: Math. Phys. Eng. Sci.*, vol. 465, no. 2107, pp. 2135–2153, 2009.
- [4] M. I. Radulescu, G. J. Sharpe, C. K. Law, and J. H. S. Lee, “The hydrodynamic structure of unstable cellular detonations,” *J. Fluid Mech.*, vol. 580, pp. 31–81, 2007.
- [5] S. Singh, J. M. Powers, and S. Paolucci, *Multidimensional Detonation Solutions from Reactive Navier-Stokes Equations*. Heidelberg, Germany: 17th Intl Colloquium on the Dynamics of Explosions and Reactive Systems, 1999.
- [6] V. N. Gamezo, A. A. Vasil’ev, A. M. Khokhlov, and E. S. Oran, “Fine cellular structures produced by marginal detonations,” *Proc. Combust. Inst.*, vol. 28, pp. 611–617, 2000.
- [7] K. Mazaheri, Y. Mahmoudi, and M. I. Radulescu, “Diffusion and hydrodynamic instabilities in gaseous detonations,” *Combust. Flame*, vol. 159, pp. 2138–2154, 2012.
- [8] Y. Mahmoudi, N. Karimi, R. Deiterding, and S. Emami, “Hydrodynamic instabilities in gaseous detonations: Comparison of Euler, Navier-Stokes, and large-eddy simulation,” *J. Propuls. Power*, vol. 30, no. 2, pp. 384–396, 2014.
- [9] X. Cai, R. Deiterding, J. Liang, M. Sun, and Y. Mahmoudi, “Diffusion and mixing effects in hot jet initiation and propagation of hydrogen detonations,” *J. Fluid Mech.*, vol. 836, p. 324–351, 2018.
- [10] B. M. Maxwell, R. R. Bhattacharjee, S. S. M. Lau-Chapdelaine, S. A. E. G. Falle, G. J. Sharpe, and M. I. Radulescu, “Influence of turbulent fluctuations on detonation propagation,” *J. Fluid Mech.*, vol. 818, pp. 646–696, 2017.
- [11] J. R. Chasnov, “Simulation of the Kolmogorov inertial subrange using an improved subgrid model,” *Phys. Fluids A Fluid Dyn.*, vol. 3, no. 1, pp. 188–200, 1991.
- [12] S. Kawai and J. Larson, “Wall-modeling in large eddy simulation: Length scales, grid resolution, and accuracy,” *Phys. Fluids*, vol. 24, p. 015105, 2012.
- [13] C. B. Kiyanda and A. J. Higgins, “Photographic investigation into the mechanism of combustion in irregular detonation waves,” *Shock Waves*, vol. 23, pp. 115–130, 2013.
- [14] J. W. Cooley and J. W. Tukey, “An algorithm for the machine calculation of complex fourier series,” *Math. Comput.*, vol. 19, pp. 297–301, 1965.
- [15] L. Massa and F. K. Lu, “The role of the induction zone on the detonation–turbulence linear interaction,” *Combust. Theory Model.*, vol. 15, no. 3, pp. 347–371, 2011.
- [16] S. G. Saddoughi and S. V. Veeravalli, “Local isotropy in turbulent boundary layers at high Reynolds number,” *J. Fluid Mech.*, vol. 268, p. 333–372, 1994.